PHYSICAL REVIEW B **91**, 180405(R) (2015)

Interfacial Dzyaloshinskii-Moriya interaction in perpendicularly magnetized Pt/Co/AlO_x ultrathin films measured by Brillouin light spectroscopy

Mohamed Belmeguenai,[1,*] Jean-Paul Adam,[2,†] Yves Roussigné,[1] Sylvain Eimer,[2] Thibaut Devolder,[2] Joo-Von Kim,[2] Salim Mourad Cherif,[1] Andrey Stashkevich,[1] and André Thiaville[3,‡]

[1]*LSPM (CNRS-UPR 3407), Université Paris 13, Sorbonne Paris Cité, 99 avenue Jean-Baptiste Clément, 93430 Villetaneuse, France*

[2]*Institut d'Electronique Fondamentale, UMR CNRS 8622, Université Paris-Sud, 91405 Orsay, France*

[3]*Laboratoire de Physique des Solides, UMR CNRS 8502, Université Paris-Sud, 91405 Orsay, France*

(Received 27 February 2015; revised manuscript received 21 April 2015; published 20 May 2015; corrected 28 May 2015)

Spin waves in perpendicularly magnetized Pt/Co/AlO_x/Pt ultrathin films with varying Co thicknesses (0.6–1.2 nm) have been studied with Brillouin light spectroscopy in the Damon-Eshbach geometry. The measurements reveal a pronounced nonreciprocal propagation, which increases with decreasing Co thickness. This nonreciprocity, attributed to an interfacial Dzyaloshinskii-Moriya interaction (DMI), is significantly stronger than asymmetries resulting from surface anisotropies for such modes. Results are consistent with an interfacial DMI constant $D_s = -1.7 \pm 0.11$ pJ/m, which favors left-handed chiral spin structures. This suggests that such films below 1 nm in thickness should support chiral states such as skyrmions at room temperature.

DOI: 10.1103/PhysRevB.91.180405 PACS number(s): 75.70.Cn, 75.40.Gb, 75.70.Tj

In the magnetism of ultrathin films, it has recently been recognized that an antisymmetric exchange known as the Dzyaloshinskii-Moriya interaction (DMI) plays an important role, even in technologically relevant sputtered polycrystalline films [1]. This interaction can appear in thin film ferromagnets in contact with a material possessing strong spin-orbit coupling. In the simplest model [2], it is of interfacial origin, and hence becomes all the more important as the film thickness decreases. The DMI modifies the statics [3,4] and dynamics [5] of domain walls, and also stabilizes chiral nanoscale bubbles known as skyrmions [6]. As a number of applications have been proposed based on domain walls, both for data storage [7] and logic gates [8]—concepts also applicable with skyrmions [6]—it is important to quantify the DMI in ultrathin films with the goal of understanding it, so as to be able to control it by tailoring material structures.

In systems of interest for spintronics applications, the DMI is not expected to be sufficiently large to overcome the exchange interaction and destabilize the uniform ferromagnetic state. In these materials, estimates of the DMI have largely been based on how this interaction modifies the properties of domain walls. Because of the underlying symmetry of the interfacial DMI, its effect can be observed in ultrathin materials with an easy anisotropy axis perpendicular to the film plane, where a transition from achiral Bloch walls (favored by dipolar interactions) to homochiral Néel walls [4,9] occurs for sufficiently large DMI. Since the DMI acts on the domain walls as an effective in-plane chiral field $\mu_0 H_{DMI} = D/M_s\Delta$, where D is the micromagnetic DMI constant and Δ the domain wall width parameter, estimates for H_{DMI} can be obtained by applying an external in-plane field so as to counterbalance the DMI field. This idea underpins several recent experimental and theoretical studies, but in each case the determination of D is at best indirect and rests upon strong assumptions involving the domain wall dynamics at hand. In particular, this has involved estimating changes in the wall energy in the creep regime [10,11], interpreting current-driven motion assisted by applied fields with a one-dimensional model [12–14], applying a droplet model to describe thermally driven edge nucleation [15], and extending the one-dimensional model to describe tilts in the domain wall structure across rectangular tracks [16]. Other techniques involving the imaging of domain walls [9] or measurements of their stray fields [17] require stabilizing domain walls in nanostructures and can only give bounds on the value of D based on whether transitions from Bloch to Néel wall profiles are seen.

Recently, a more direct measurement of D through frequency shifts of oppositely propagating spin waves (SW) was proposed [18] and demonstrated experimentally for Pt/Co/Ni [19], Pt/NiFe [20,21], and Pt/CoFeB [22] films. Indeed, when the magnetization and wave vector are both in plane and perpendicular to each other, the chiral DMI interaction results in nonreciprocal SW propagation that manifests itself as a linear wave vector dependence of the SW frequencies. In this Rapid Communication, we study ultrathin Pt/Co/AlO_x multilayers with perpendicular anisotropy, a system for which D has been inferred to be very large based on previous experiments on domain walls [15,17] and on *ab initio* calculations [23,24]. We show that the large Gilbert damping ($\alpha \sim 0.1$–0.3) known for such systems [25] is not an impediment for characterizing nonreciprocal SW propagation, since the frequency shifts are larger than the typical spectral linewidths of the SW peaks. Our precise estimates of the DMI for a series of samples where the cobalt thickness is changed allow us to quantitatively establish the interfacial nature of DMI. Moreover, the absolute sign of the DMI is also determined to be negative (i.e., favoring left-handed magnetization cycloids [12]), in agreement with domain wall experiments [12,15,17].

Co ultrathin films with thickness varying from 0.6 to 1.2 nm were grown by sputtering in an argon pressure of 2.5×10^{-3} mTorr on Si/SiO_2 substrates buffered with a Ta(3 nm)/Pt(3 nm) bilayer, and then capped with AlO_x (2 nm)/Pt (3 nm) bilayer. In this system, the Pt bottom layer induces perpendicular magnetic anisotropy and DMI in the

*belmeguenai.mohamed@univ-paris13.fr
†jean-paul.adam@u-psud.fr
‡andre.thiaville@u-psud.fr

TABLE I. Magnetic parameters obtained from the best fits of BLS results with the model described below, using the saturation magnetization from magnetometry and $g = 2.17$. The absolute values of D_{eff} and D_s are given.

t (nm)	$\mu_0 M_s$ (T)	$\mu_0 H_{\text{sat}}$ MOKE (T)	$\mu_0 H_{K_{\text{eff}}}$ BLS (T)	D_{eff} (mJ/m^2)	D_s (pJ/m)
0.6	1.38	0.95	1.03	2.71 ± 0.16	1.63 ± 0.1
0.8	1.48	0.82	0.87	2.18 ± 0.25	1.75 ± 0.2
0.9	1.51	0.75	0.68	1.88 ± 0.08	1.69 ± 0.07
0.95	1.68	0.51	0.36	1.76 ± 0.24	1.67 ± 0.23
1.2	1.71	0.10	0.11	1.57 ± 0.18	1.88 ± 0.22

ultrathin Co layer, whereas the AlO_x cap layer is thought to only induce perpendicular anisotropy. All experiments have been performed at room temperature. Magnetometry [alternating gradient force magnetometer (AGFM) and superconducting quantum interference device (SQUID)] has been used to measure the hysteresis loops of the samples, with the field applied perpendicular to the sample plane, and to determine the magnetization at saturation M_s. For the thicker samples, M_s is similar to that of the bulk Co while that for the thinnest film is significantly smaller but remains in the range measured by Metaxas *et al.* [26] (Table I). The polar magneto-optical Kerr effect (p-MOKE) has been used to obtain the hysteresis loops with the magnetic field applied along the normal and in the plane of the sample (as shown in Fig. 1). The Kerr rotation at saturation is deduced from the hysteresis loops obtained with the field applied perpendicular to the plane. This amplitude signal is then used to normalize the measured Kerr rotation while the field is applied in the sample plane (Fig. 1). The normalized signal is ~ 1 for all the samples, ensuring a macrospin behavior during the magnetization reversal, and the effective anisotropy fields are then obtained from the hysteresis loops by fitting with the Stoner-Wohlfarth model [27]. The obtained values are summarized in Table I. All samples exhibit a perpendicular magnetic anisotropy that increases with decreasing Co thickness.

Brillouin light spectroscopy (BLS) gives access to SW modes with nonzero wave vectors. The SW in the film inelastically scatter the light from an incident laser beam. The frequency shift is analyzed using a 2×3 pass Fabry-Pérot interferometer, which typically gives access to a 3–300 GHz spectral frequency range. For the used backscattering study, the investigated spin-wave vector lies in the plane of incidence and its length is $k_{\text{sw}} = 4\pi \sin(\theta_{\text{inc}})/\lambda$ (with θ_{inc} the angle of incidence and $\lambda = 532$ nm the wavelength of the illuminating laser). Therefore, it can be swept in the 0–20 μm^{-1} interval through the rotation of the sample around a planar axis. The magnetic field was applied perpendicular to the incidence plane, which allows spin waves propagating along the in-plane direction perpendicular to the applied field to be probed [Damon-Eshbach (DE) geometry]. For each angle of incidence, the spectra were obtained after counting photons up to 15 h (especially for the highest incidence angles) to have well-defined spectra where the line position can be determined with accuracy better than 0.1 GHz. The Stokes (S, negative frequency shift relative to the incident light as a SW was created) and anti-Stokes (AS, positive frequency shift relative to the incident light as a SW was absorbed) frequencies were then determined from Lorentzian fits to the BLS spectra. In the following, as we refer to the properties of the SW, f_S denotes the absolute value of the Stokes frequency, and wave vectors along that of the photons are counted positive.

The BLS measurements were performed with the magnetization saturated in the film plane under magnetic fields

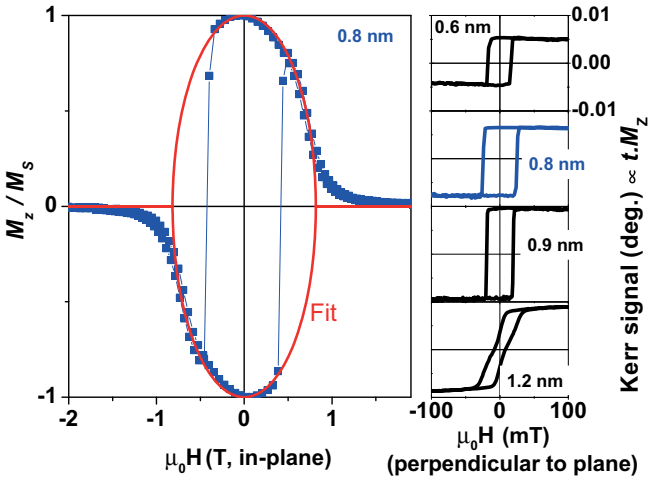

FIG. 1. (Color online) Polar MOKE magnetometry for Pt/Co(t)/AlO_x samples of different thicknesses t. Left panel: Experimental (symbols) and fitted (red bold line) hysteresis loops of the perpendicular component of the magnetization vs in-plane applied magnetic field for the $t = 0.8$ nm sample. Right panels: Hysteresis loops of some representative samples for fields applied perpendicularly to the sample plane.

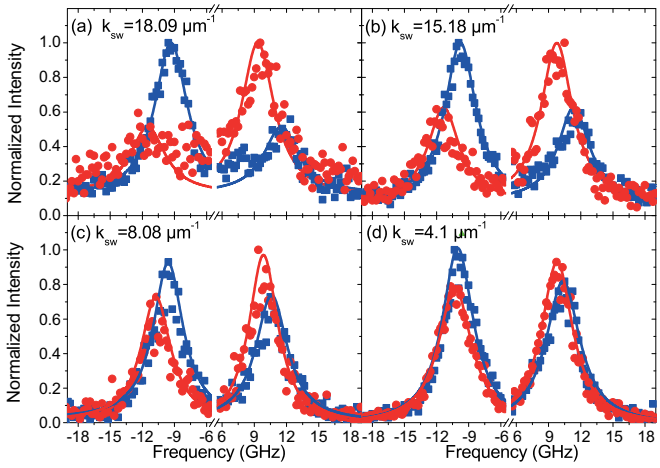

FIG. 2. (Color online) BLS spectra measured for Pt/Co(1.2 nm)/AlO_x at two different applied field values $\mu_0 H = 0.4$ T (-0.4 T) in blue squares (red circles) and at four characteristic light incidence angles corresponding to $k_{\text{sw}} = 18.09$, 15.18, 8.08, and 4.1 μm^{-1}. Symbols refer to the experimental data and solid lines are the Lorentzian fits.

above the saturation fields deduced from the MOKE loops (shown in Table I). Figure 2 shows typical BLS spectra for the 1.2 nm thick sample for $k_{sw} = 18.09$, 15.18, 8.08, and 4.1 μm^{-1} corresponding to incidence angles $\theta_{inc} = 50°$, 40°, 20°, and 10°, under an applied field $\mu_0 H = 0.4$ T. Importantly, mirror-symmetrical results were obtained for $\mu_0 H = -0.4$ T, as expected from nonreciprocity. Beside the well-known intensity asymmetry of the S and AS modes due to the coupling mechanism between the light and SWs (in thin films), an unusually pronounced difference between the frequencies of both modes (nonreciprocity), especially for higher values of k_{sw}, is revealed by these spectra. Various mechanisms, in particular, perpendicular uniaxial surface anisotropy and DMI, can induce this frequency difference between the DE Stokes and anti-Stokes lines. However, an effect of interface anisotropy is observable only if the characteristic DE spatial asymmetry (of the dynamic magnetization distribution across the film) is sufficiently pronounced, in other words, in relatively thick films such that $k_{sw}t$ is not much smaller than unity. The frequency difference present in our samples is, despite the large interface anisotropy of Pt/Co/AlO_x, much larger than what is expected from different surface anisotropies at the two interfaces of the ferromagnetic film [21]. We note also that the DMI effects seen are much larger than what was measured on perpendicularly magnetized Pt/CoFeB [22] and in-plane magnetized Pt/Co/Ni [19] ultrathin films.

The variation of the frequencies of the S and AS modes as a function of the spin-wave wave vector is shown in Fig. 3(a) (for the sake of clarity, the data for the $t = 0.95$ nm sample are not presented). The prominent feature of these dispersion curves is their asymmetry with respect to $k_{sw} = 0$. The frequency difference $\Delta f = f_S - f_{AS}$ is plotted in Fig. 3(b) as a function of k_{sw}, revealing a linear dependence with a slope that changes markedly with Co thickness. For the samples studied here and for positive field, the AS mode frequency f_{AS} was found to be always higher than f_S, as shown on Fig. 3. It is worth noting that BLS measurements of Δf as a function of H [see the inset of Fig. 3(b)] reveal that Δf is independent of the applied field, as expected from the model mentioned below and similarly to previous work [19].

The BLS data have been analyzed using an analytical model relevant for ultrathin films [19,28,29], where the DE mode frequencies are given by

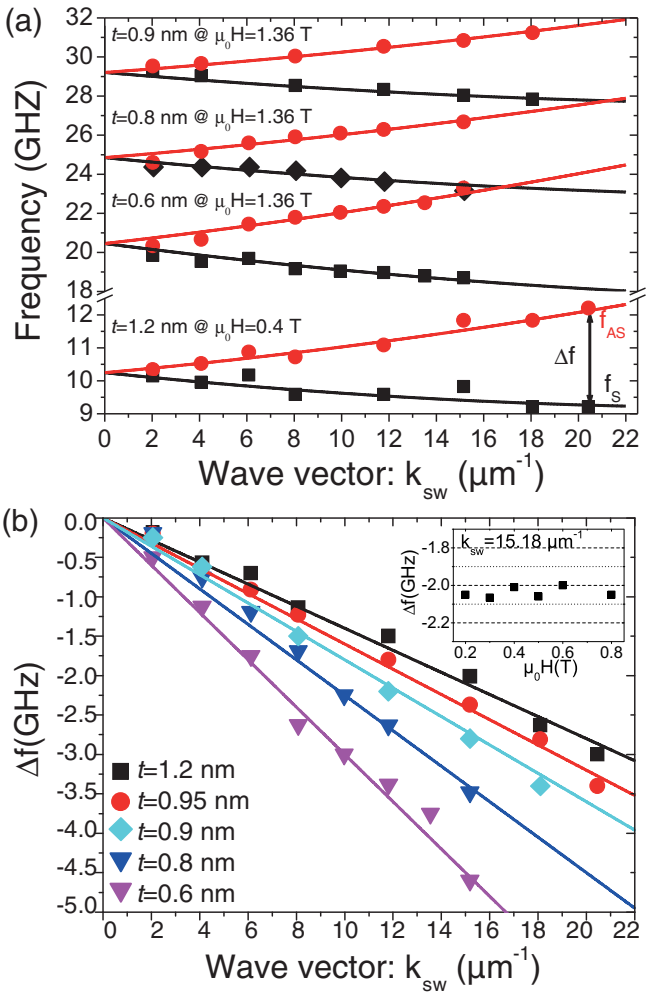

FIG. 3. (Color online) (a) Measured spin-wave dispersion for various Co thicknesses t. Symbols show the experimental BLS data for AS (red, with k_{sw} inverted) and S frequencies (black). Solid lines represent the model described by Eq. (1) with effective DMI constants D_{eff} and magnetic parameters given in Table I. (b) Wave vector (k_{sw}) dependence of experimental frequency difference Δf (symbols) compared to the DMI model (solid curves). The inset shows the measured dependence of Δf vs the applied magnetic field in the case of the $t = 1.2$ nm sample at a fixed wave vector value $k_{sw} = 15.18$ μm^{-1}.

$$f = f_0 \pm f_{DMI} \equiv \frac{\gamma \mu_0}{2\pi}\sqrt{\left[H + Jk_{sw}^2 + P(k_{sw}t)M_s\right]\left[H + Jk_{sw}^2 - P(k_{sw}t)M_s - H_{K_{eff}}\right]} \pm \frac{\gamma}{\pi M_s} D_{eff} k_{sw}. \quad (1)$$

Here, H represents the in-plane applied field, M_s the saturation magnetization of Co, γ the absolute value of the gyromagnetic ratio [$\gamma/(2\pi) = g \times 13.996$ GHz/T, with g the Landé factor], μ_0 the vacuum permeability, $J = \frac{2A}{\mu_0 M_s}$ the SW stiffness (also called D in the SW literature) with A the micromagnetic exchange constant, D_{eff} the effective micromagnetic DMI constant, H_K the perpendicular uniaxial anisotropy field, $H_{K_{eff}} = H_K - M_s$ the effective anisotropy field, and $P(k_{sw}t) = 1 - \frac{1-\exp(-|k_{sw}|t)}{|k_{sw}|t}$. In Eq. (1), the signs of D and k_{sw} have been kept, H is the absolute field and $\pm$ its sign, according to the convention detailed below. If DMI is of purely interfacial origin, one expects a variation with thickness according to $D_{eff}(t) = D_s/t$. From this, the frequency difference can be deduced to be

$$\Delta f = f_S - f_{AS} = \frac{2\gamma}{\pi M_s} D_{eff} k_{sw} = \frac{2\gamma}{\pi} k_{sw} \frac{D_s}{M_s t}, \quad (2)$$

where the last equality stresses that in fact D_s is the directly determined quantity, which is independent of the uncertainties in the film thickness t. The experimental data were fitted

conjointly by Eqs. (1) and (2) by using the values of $M_s t$ determined from magnetometry and the bulk value $g = 2.17$ to determine the different parameters summarized in Table I. We note that the strength of the DMI found is largely insensitive to whether the exchange constant A is assumed or fitted from the data, as different deformations of the dispersion curves are controlled by these parameters. For $t = 0.6$ nm, D_{eff} is in good agreement with the value $D = -2.2$ mJ/m^2 obtained by Ref. [15] from domain wall experiments. The variations of D_{eff} with t are consistent, to 10% accuracy, with a single value for D_s. It is also worth mentioning that the values of the saturation field in the sample plane, deduced from fits of the BLS data, are in very good agreement with those deduced from the MOKE hysteresis loops, (compare H_{sat} and $H_{K_{\text{eff}}}$ in Table I). This shows that any second-order anisotropy term can be neglected, and that the assumed value of g is consistent with our findings.

Finally, we stress that the *sign* of the DMI can be also determined. Indeed, performing the calculation leading to Eq. (1) shows that, when the transferred optical wave vector (along x), the applied field (along y), and the film normal from Pt to Co (along z) form a right-handed reference frame, the Stokes SW corresponds to a left-handed cycloid. As we measured in this configuration and found that $f_{\text{AS}} > f_{\text{S}}$, this means that DMI is negative, i.e., left-handed cycloids are favored.

In conclusion, Pt/Co/AlO$_x$/Pt ultrathin films with perpendicular magnetization comprising various Co thicknesses have been studied by Brillouin light spectroscopy and magnetometry. The analysis of the BLS spectral reveals that the observed large nonreciprocities in the spin-wave dispersion are consistent with a single surface DMI constant of $D_s = -1.7 \pm 0.11$ pJ/m. The sign of DMI implies that left-handed cycloidal spin structures are favored, which is consistent with conclusions from domain wall experiments [12,15] and with *ab initio* calculations [23,24].

The authors would like to thank M. Kostylev and P. Moch for fruitful discussions, P. Balestrière for help with the sample preparation, and J.-L. Cercus and L. Fruchter for help in SQUID measurements. This work has been partially supported by the Agence Nationale de la Recherche through contracts ANR-11-BS10-0003 (NanoSWITI) and ANR-14-CE26-0012 (ULTRASKY), and by the Conseil Régional, Île-de-France through the DIM C'Nano (IMADYN project).

[1] A. Brataas, Nat. Nanotechnol. **8**, 485 (2013).
[2] A. Fert, Mater. Sci. Forum **59-60**, 439 (1990).
[3] I. E. Dzyaloshinskii, J. Exptl. Theoret. Phys. (USSR) **47**, 992 (1964) [Sov. Phys. JETP **20**, 665 (1965)].
[4] M. Heide, G. Bihlmayer, and S. Blügel, Phys. Rev. B **78**, 140403 (2008).
[5] A. Thiaville, S. Rohart, É. Jué, V. Cros, and A. Fert, Europhys. Lett. **100**, 57002 (2012).
[6] A. Fert, V. Cros, and J. Sampaio, Nat. Nanotechnol. **8**, 152 (2013).
[7] S. S. P. Parkin, M. Hayashi, and L. Thomas, Science **320**, 190 (2008).
[8] D. A. Allwood, G. Xiong, C. C. Faulkner, D. Atkinson, D. Petit, and R. P. Cowburn, Science **309**, 1688 (2005).
[9] G. Chen, J. Zhu, A. Quesada, J. Li, A. T. N'Diaye, Y. Huo, T. P. Ma, Y. Chen, H. Y. Kwon, C. Won, Z. Q. Qiu, A. K. Schmid, and Y. Z. Wu, Phys. Rev. Lett. **110**, 177204 (2013).
[10] S.-G. Je, D.-H. Kim, S.-C. Yoo, B.-C. Min, K.-J. Lee, and S.-B. Choe, Phys. Rev. B **88**, 214401 (2013).
[11] A. Hrabec, N. A. Porter, A. Wells, M. J. Benitez, G. Burnell, S. McVitie, D. McGrouther, T. A. Moore, and C. H. Marrows, Phys. Rev. B **90**, 020402 (2014).
[12] S. Emori, U. Bauer, S.-M. Ahn, E. Martinez, and G. S. D. Beach, Nat. Mater. **12**, 611 (2013).
[13] K.-S. Ryu, S.-H. Yang, L. Thomas, and S. S. P. Parkin, Nat. Commun. **5**, 3910 (2014).
[14] J. Torrejon, J. Kim, J. Sinha, S. Mitani, M. Hayashi, M. Yamanouchi, and H. Ohno, Nat. Commun. **5**, 4655 (2014).
[15] S. Pizzini, J. Vogel, S. Rohart, L. D. Buda-Prejbeanu, E. Jué, O. Boulle, I. M. Miron, C. K. Safeer, S. Auffret, G. Gaudin, and A. Thiaville, Phys. Rev. Lett. **113**, 047203 (2014).
[16] O. Boulle, S. Rohart, L. D. Buda-Prejbeanu, E. Jué, I. M. Miron, S. Pizzini, J. Vogel, G. Gaudin, and A. Thiaville, Phys. Rev. Lett. **111**, 217203 (2013).
[17] J.-P. Tetienne, T. Hingant, L. J. Martinez, S. Rohart, A. Thiaville, L. H. Diez, K. Garcia, J.-P. Adam, J.-V. Kim, J.-F. Roch, I. M. Miron, G. Gaudin, L. Vila, B. Ocker, D. Ravelosona, and V. Jacques, Nat. Commun. **6**, 6733 (2015).
[18] D. Cortés-Ortuño and P. Landeros, J. Phys.: Condens. Matter **25**, 156001 (2013).
[19] K. Di, V. L. Zhang, H. S. Lim, S. C. Ng, M. H. Kuok, J. Yu, J. Yoon, X. Qiu, and H. Yang, Phys. Rev. Lett. **114**, 047201 (2015).
[20] H. T. Nembach, J. M. Shaw, M. Weiler, É. Jué, and T. J. Silva, arXiv:1410.6243.
[21] A. A. Stashkevich, M. Belmeguenai, Y. Roussigné, S. M. Cherif, M. Kostylev, M. Gabor, D. Lacour, C. Tiusan, and M. Hehn, arXiv:1411.1684.
[22] K. Di, V. L. Zhang, H. S. Lim, S. C. Ng, M. H. Kuok, X. Qiu, and H. Yang, Appl. Phys. Lett. **106**, 052403 (2015).
[23] F. Freimuth, S. Blügel, and Y. Mokrousov, J. Phys.: Condens. Matter **26**, 104202 (2014).
[24] H. Yang, A. Thiaville, S. Rohart, A. Fert, and M. Chshiev, arXiv:1501.05511.
[25] A. J. Schellekens, L. Deen, D. Wang, J. T. Kohlhepp, H. J. M. Swagten, and B. Koopmans, Appl. Phys. Lett. **102**, 082405 (2013).
[26] P. J. Metaxas, J. P. Jamet, A. Mougin, M. Cormier, J. Ferré, V. Baltz, B. Rodmacq, B. Dieny, and R. L. Stamps, Phys. Rev. Lett. **99**, 217208 (2007).
[27] V. Grolier, J. Ferré, A. Maziewski, E. Stefanowicz, and D. Renard, J. Appl. Phys. **73**, 5939 (1993).
[28] J.-H. Moon, S.-M. Seo, K.-J. Lee, K.-W. Kim, J. Ryu, H.-W. Lee, R. D. McMichael, and M. D. Stiles, Phys. Rev. B **88**, 184404 (2013).
[29] M. Kostylev, J. Appl. Phys. **115**, 233902 (2014).